Transmission coefficient calculation using the derived inelastic transport analogy of the transmission matrix method; application to tunnelling into a marginal Fermi liquid

1998 J. Phys.: Condens. Matter 10 327

(http://iopscience.iop.org/0953-8984/10/2/012)

J. Phys.: Condens. Matter **10** (1998) 327–339. Printed in the UK PII: S0953-8984(98)86038-4

Transmission coefficient calculation using the derived inelastic transport analogy of the transmission matrix method; application to tunnelling into a marginal Fermi liquid

Martin Kupka†

Institute of Experimental Physics, Slovak Academy of Sciences, Watsonova 47, 04353 Košice, Slovakia

Received 15 July 1997

Abstract. An expression for the probability of transmission of an electron from an ordinary metal into a medium with a finite quasiparticle lifetime is derived. The derivation is based on using a certain matrix, analogous to the transmission matrix for the elastic transport case, assigned to each region of the sample being investigated. This matrix is determined by the functional shapes of the electronic reciprocal-effective-mass tensor, the one-particle potential energy and the retarded self-energy in a given sample region, as well as by the energy and direction of motion of the incident electron.

As an example of an application, the differential conductance is calculated for a tunnelling contact between an ordinary metal and an anisotropic marginal-Fermi-liquid metal for various characters of the contact interlayer zone.

1. Introduction

The quantum-mechanical electronic transmission coefficient, representing the probability of transmission of an electron from one electrode through the vacuum or some solid-state structures into another electrode, plays an important role in a variety of physical problems. For example, it occurs in various forms of Landauer's formula, allowing one to calculate the conductance of a sample from its transmissive behaviour [1–3], in an expression for the current in scanning tunnelling microscope theory [4], and in formulas for the differential conductance in some approaches to tunnelling spectroscopy or point-contact spectroscopy theory (see, e.g., [5]). In all of these cases, to predict the results theoretically or to interpret experimental data it is necessary to calculate the transmission coefficients for particular situations.

In the case of elastic electronic transport through layered planar structures, i.e. when the system parameters (electronic effective mass, potential energy) are varying only in one spatial direction and the behaviour of an electron can be described by a one-electron wave function governed by the one-electron Schrödinger equation, there is an efficient method for calculating the electronic transmission coefficient—the so-called 'transmission matrix approach' [6].

In this approach, a certain matrix (called a 'transmission matrix') is assigned to each sample region with constant electronic effective mass and potential energy. This matrix is

† E-mail: kupkam@linux1.saske.sk.

0953-8984/98/020327+13$19.50

determined only by the effective-mass and potential-energy values in the region considered, and the energy of an incident electron. The matrix connects the values of a wave function and its derivative at the two ends of a given region. Any real smooth potential-energy and effective-mass functions are approximated by multistep functions having N segments. Each one of these segments represents a single region with constant parameters. The transmission matrix is calculated for each such segment. The overall transmission matrix is found by multiplying the transmission matrices for all partial segments. This overall matrix is used for calculating the transmission coefficient.

However, very often the behaviour of one particle in a many-particle system is described by means of a one-particle Green's function instead of a one-particle wave function. The marginal-Fermi-liquid model represents an important illustration of such a situation.

Marginal-Fermi-liquid (MFL) phenomenology [7, 8] was proposed to correlate many normal-state properties of high-temperature superconductors as well as the appearance of a Fermi surface by means of a single hypothesis. In this approach, the crucial role is played by a strongly energy-dependent and momentum-independent retarded one-particle self-energy of a special form. The imaginary part of this self-energy reveals itself in, for example, tunnelling experiments.

Within the Green's function formalism, in some cases the quasiparticle energies can be evaluated by solving the so-called 'effective wave equation' for the auxiliary 'wave function'. This 'effective wave equation' is obtained from the original Green's function equation of motion (with the self-energy given *a priori*) by replacing the Green's function (a function of two space-time points) by an auxiliary 'wave function' (a function of only one space-time point) and putting the right-hand side of the equation equal to zero [9].

In general, if the self-energy is a complex function of the energy (with a non-zero imaginary part), the 'effective wave equation' represents a non-linear non-Hermitian problem. In such a case it is impossible to use the bilinear expansion of the Green's function in auxiliary 'wave functions'. Then it is not permissible to interpret and treat the auxiliary 'wave function' as a real one-particle wave function and the 'effective wave equation' as a Schrödinger equation describing the quasiparticle behaviour, with all the corresponding consequences [9]. So, we cannot use the simpler wave-function formalism for investigating the electron tunnelling. We are forced to deal with more complicated Green's function formalism to evaluate the quantities needed.

In the present paper we are dealing with inelastic electronic transport through a layered planar structure, so the behaviour of an electron is described by a one-electron retarded Green's function with a finite self-energy imaginary part. To take into account possible lattice anisotropy we also introduce into our consideration the anisotropic reciprocal-effective-mass (REM) tensor.

The method derived retains the advantages and efficiency of the 'elastic' 'transmission matrix approach'. The transmission coefficient is also calculated by means of a certain matrix (analogous to the transmission matrix), assigned to each region of the sample. This matrix is unambiguously determined by the functional shapes of the REM tensor, the potential energy and the self-energy within a given sample region, and by the energy and the direction of an incident electron. If the many-particle effects are negligible, i.e. the self-energy vanishes, our matrix becomes identical with the conventional transmission matrix. The structure of our matrix enables us to express the entire matrix as a product of particular matrices assigned to the sub-regions of the region considered. So it is possible to use efficient numerical procedures for evaluating the transmission coefficients for various solid-state structures or to make some deductions about the effects of particular barriers on the total transmission probabilities, and so on.

A slightly different method leading to the same result (the same matrix) was used in a very abridged and less consistent form in our earlier article [10].

As an illustrative example of the applicability of the method presented, the differential conductance for tunnelling contact between an ordinary metal and an anisotropic MFL metal was calculated for different situations (various orientations of the symmetry axes with respect to the interface, various functional forms of the transitions of model characteristics from ordinary-metal bulk parameters into the MFL ones, etc).

Although initially developed for MFLs, the method presented can be used for calculating the transmission coefficients not only for MFLs, but also for any system with momentum-independent self-energy (momentum independence reflects strongly spatially localized interactions), e.g. heavy-fermion compounds [11].

2. Theoretical derivation of an expression for the electronic transmission coefficient

To study the probability of the transmission of an electron from an ordinary metal to some material of interest, we consider a model system represented by a sample consisting of a macroscopic electrode made from the material of interest and filling up the whole half-space, with a 'barrier' layer and an ordinary-metal layer of macroscopic thickness (serving as the other electrode) deposited on its planar surface (parallel with the xy-plane). Because this geometry has been adopted, the physical properties of our sample are expected to vary only in the direction perpendicular to the layers, i.e. they are functions only of the coordinate z. With respect to the spatial changes of these properties, the sample can be divided into three principal regions (ignoring the changes near the free surface of an ordinary-metal electrode which are irrelevant for the phenomena investigated, due to the macroscopic electrode thickness): the region of constant bulk ordinary-metal parameters for $-L \leqslant z < 0$; the interlayer region with varying parameters for $0 \leqslant z \leqslant Z$; and the region of the material being investigated with constant bulk parameters for $Z < z < \infty$. In the interlayer region the parameters vary from those of the first region to the ones of the third region. The changes need not be continuous; jumps can occur. The interlayer region contains, besides an 'artificial' barrier layer, also several 'degraded' surface atomic layers of the two electrodes.

We suppose that the low-temperature behaviour of an electron in the above-mentioned model system is described by a one-electron zero-temperature retarded Green's function. As we are interested in non-ferromagnetic materials and situations without an external magnetic field, the Green's function is a diagonal matrix in the spin space and so we will omit the spin indices. The relevant model parameters are those occurring in the Green's function: the 'band' reciprocal-effective-mass tensor $1/\mathbf{m}(z)$, the one-electron potential energy $U(z)$ and the retarded self-energy $\Sigma(E; z, z')$. In our approach we assume that these characteristic parameters are known.

The 'band' REM tensor is introduced to take into account the symmetry of a crystalline lattice. The 'band' attributes reflect the fact that this tensor reflects only the interaction of an electron with the static lattice (with a periodic potential field) and no many-electron effects or corrections are considered. For the elements of the REM tensor we use the notation $(1/\mathbf{m})_{ij} \equiv 1/m_{ij}$.

Many-particle effects are included in the self-energy term. We are interested in systems with momentum-independent bulk self-energy (see the introduction). This reflects strongly spatially localized interactions. We suppose that this strong localization persists also in the surface layers, but that the 'amplitude' of these processes can change. So we assume that within the interlayer region the self-energy term has the form $\Sigma(E, z)\delta(z - z')$, where $\delta(z)$

is the Dirac delta function. In an ordinary metal no many-particle effects are expected, so in this part of the sample the self-energy vanishes.

The one-electron potential-energy term $U(z)$ describes the electron potential-energy changes due to the applied external electric field, the 'artificial' barrier layer, degradation of the near-interface layers, etc.

As a starting point for calculating the transmission coefficient, we use the relation

$$P(f,i) \equiv |\langle f|i\rangle|^2. \tag{1}$$

The quantity $P(f,i)$ can be interpreted as a probability of a sudden transition of the system from the normalized state $|i\rangle$ to the normalized state $|f\rangle$. With respect to the goals that we want to achieve (to calculate the probability of transmission of one electron from an ordinary-metal electrode to the electrode made of the metal being investigated, the rest of the system remaining unchanged), we write these state vectors in the form

$$|\xi\rangle \equiv \left(\sum_m |m, N+1\rangle\langle m, N+1|c_\xi^+|0, N\rangle\right) \Big/ \sqrt{\sum_m |\langle m, N+1|c_\xi^+|0, N\rangle|^2}$$
$$\text{for } E \leqslant E_m(N+1) - E_0(N) \leqslant E + \mathrm{d}E. \tag{2}$$

Here the $|m, N\rangle$ are the exact normalized N-electron eigenstates of the Hamiltonian describing our model system and the $E_m(N)$ are the exact energies of the system in these states. The value $m = 0$ is reserved for quantities belonging to the ground state. The operator c_ξ^+, $\xi = i, f$, defined as

$$c_\xi^+ \equiv \int \mathrm{d}V\ \varphi_\xi(\boldsymbol{r})\Psi^+(\boldsymbol{r}) \tag{3}$$

creates the electron in a one-electron state $\varphi_\xi(\boldsymbol{r})$. $\Psi^+(\boldsymbol{r})$ is an obvious 'field' operator creating an electron at a point $\boldsymbol{r}$. The integration in (3) runs over the volume of the sample.

The vector $|\xi\rangle$ can be interpreted as a state vector corresponding to the following situation: an N-electron system is in its ground state and an 'additional' electron is in the state $\varphi_\xi(\boldsymbol{r})$ and has an energy $E \geqslant E_F$ (in the sense that the energy of the whole $(N+1)$-electron system is $E_m(N+1) = E_0(N) + E$). E_F is the Fermi energy of the N-electron system: $E_F \equiv E_0(N+1) - E_0(N)$. To obtain the 'pure' probability of an electron transmission from one state to another (without complications connected with the 'creation' of the states considered), the vector $|\xi\rangle$ is normalized to unity.

Now we need to express the relation (1) in terms of the retarded one-electron Green's function $G(t-t'; f, i)$, defined in the usual way:

$$G(t-t'; f, i) \equiv -\mathrm{i}\theta(t-t')\langle 0, N|\left[c_f(t)c_i^+(t') + c_i^+(t')c_f(t)\right]|0, N\rangle. \tag{4}$$

Here $\theta(t)$ is a step function ($\theta(t) = 1$ for $t \geqslant 0$, $\theta(t) = 0$ otherwise). $c_\xi^+(t)$ is the Heisenberg representation of the operator c_ξ^+.

Comparing the form of the spectral representation of $G(E; f, i)$ (the Fourier transform of $G(t-t'; f, i)$ in $t-t'$) (see, e.g., [12]) with the structure of our states (2), we see that $P(f,i)$ can be expressed as

$$P(E; f, i) = \frac{|G(E; f, i) - G^*(E; i, f)|^2}{4\,\mathrm{Im}\,G(E; f, f)\,\mathrm{Im}\,G(E; i, i)}. \tag{5}$$

To evaluate this expression we need to know the Green's function. The retarded one-electron Green's function for the above-described model system obeys the equation (in the $\boldsymbol{r}$-representation)

$$\left[E + \frac{\hbar^2}{2}\boldsymbol{\nabla}\cdot\left(\frac{1}{\mathbf{m}(z)}\right)\cdot\boldsymbol{\nabla} - U(z) - \Sigma(E,z)\right]G(E; \boldsymbol{r}_\parallel - \boldsymbol{r}'_\parallel, z, z') = \hbar\delta(\boldsymbol{r}-\boldsymbol{r}'). \tag{6}$$

As in the case investigated the Green's function is a function of $\boldsymbol{r}_\parallel - \boldsymbol{r}'_\parallel$, equation (6) can be rewritten in the form

$$\left[E + \frac{\overline{h}^2}{2}\frac{\partial}{\partial z} D_z(\boldsymbol{q}_\parallel, z) + \frac{\mathrm{i}\overline{h}^2}{2}\left(\frac{q_x}{m_{zx}(z)} + \frac{q_y}{m_{zy}(z)}\right)\frac{\partial}{\partial z} - E_\parallel(\boldsymbol{q}_\parallel, z) - U(z) - \Sigma(E, z)\right] \times G(E, \boldsymbol{q}_\parallel; z, z') = \overline{h}\delta(z - z'). \tag{7}$$

Here $G(E, \boldsymbol{q}_\parallel; z, z')$ is the partial Fourier transform of the Green's function $G(E, \boldsymbol{r}_\parallel - \boldsymbol{r}'_\parallel; z, z')$ and satisfies the following boundary conditions:

$$G(E + \mathrm{i}0^+, \boldsymbol{q}_\parallel; \pm\infty, z') = 0. \tag{8}$$

The energy $E_\parallel(\boldsymbol{q}_\parallel, z)$ is defined as

$$E_\parallel(\boldsymbol{q}_\parallel, z) \equiv \frac{\overline{h}^2}{2}\left(\frac{q_x^2}{m_{xx}(z)} + 2\frac{q_x q_y}{m_{xy}(z)} + \frac{q_y^2}{m_{yy}(z)}\right).$$

To abbreviate the notation, we introduced the operator $D_z(\boldsymbol{q}_\parallel, z)$ defined as

$$D_z(\boldsymbol{q}_\parallel, z) \equiv \mathrm{i}\left(\frac{q_x}{m_{zx}(z)} + \frac{q_y}{m_{zy}(z)}\right) + \frac{1}{m_{zz}(z)}\frac{\partial}{\partial z}. \tag{9}$$

The solution of equation (7) can be written in the form [13]

$$G(\mathrm{EQ}; z, z') = \frac{2}{\overline{h}}\frac{(1 - \theta(z - z'))f_<(\mathrm{EQ}; z)f_>(\mathrm{EQ}; z') + \theta(z - z')f_>(\mathrm{EQ}; z)f_<(\mathrm{EQ}; z')}{f_<(\mathrm{EQ}; z')D_z(\boldsymbol{q}_\parallel, z')f_>(\mathrm{EQ}; z') - f_>(\mathrm{EQ}; z')D_z(\boldsymbol{q}_\parallel, z')f_<(\mathrm{EQ}; z')} \tag{10}$$

where $\mathrm{EQ} = E, \boldsymbol{q}_\parallel$ in this expression. Both f-functions obey the common equation (7) with zero right-hand side and each one satisfies just one boundary condition:

$$f_<(E + \mathrm{i}0^+, \boldsymbol{q}_\parallel; -\infty) = 0 \tag{11a}$$

$$f_>(E + \mathrm{i}0^+, \boldsymbol{q}_\parallel; +\infty) = 0. \tag{11b}$$

Taking into account the boundary condition (11), the f-functions have the following forms for $z < 0$, i.e. the region of constant ordinary-metal bulk parameters:

$$f_<(E, \boldsymbol{q}_\parallel; z) = \exp(\mathrm{i}q_z^n z) \qquad \text{for } z < 0 \tag{12a}$$

$$f_>(E, \boldsymbol{q}_\parallel; z) = a\exp(\mathrm{i}q_z^p z) + b\exp(\mathrm{i}q_z^n z) \qquad \text{for } z < 0. \tag{12b}$$

The coefficients a and b are chosen in such a way that the full solution $f_>$ satisfies the boundary condition at $+\infty$.

The wave-vector components are of the form

$$q_z^{p(n)}(E, \boldsymbol{q}_\parallel) = -\left(q_x\frac{m_{zz}^0}{m_{zx}^0} + q_y\frac{m_{zz}^0}{m_{zy}^0}\right) \pm \frac{m_{zz}^0 v_z^0(E, \boldsymbol{q}_\parallel)}{\overline{h}}$$

$$v_z^0(E, \boldsymbol{q}_\parallel) = \sqrt{\frac{2(E - E_\parallel^0(\boldsymbol{q}_\parallel) - U_0)}{m_{zz}^0} + \overline{h}^2\left(\frac{q_x}{m_{zx}^0} + \frac{q_y}{m_{zy}^0}\right)^2}.$$

v_z^0 is the absolute value of the z-component of the electron group velocity in an ordinary metal. The superscript p indicates the wave-vector component with the plus sign before the group velocity term, while the superscript n indicates that with the minus sign. If m_{zz}^0 is positive, q_z^p corresponds to the state with the positive z-component of the electron group velocity and q_z^n to the state with the negative one. For brevity, the dependence of q_z and v_z^0 on E and $\boldsymbol{q}_\parallel$ is not written out explicitly in the following.

The quantity $P(f,i)$, equation (1), represents the reflection coefficient if the initial state $\varphi_i(\boldsymbol{r})$ is chosen in the planar-wave form describing an electron moving with a velocity that is the positive z-component of a group velocity from an ordinary-metal electrode to the interface and the final state $\varphi_f(\boldsymbol{r})$ is chosen in the planar-wave form describing an electron moving with a velocity that is the z-component of a negative group velocity from the interface to the ordinary-metal electrode. So the initial and final states are chosen in the forms

$$\varphi_i(\boldsymbol{q}_\parallel, z) = \frac{1}{\sqrt{L}} \exp(\mathrm{i}p_z^p z)(1-\theta(z))\delta(\boldsymbol{q}_\parallel - \boldsymbol{k}'_\parallel) \tag{13a}$$

$$\varphi_f(\boldsymbol{q}_\parallel, z) = \frac{1}{\sqrt{L}} \exp(\mathrm{i}p_z^n z)(1-\theta(z))\delta(\boldsymbol{q}_\parallel - \boldsymbol{k}_\parallel) \tag{13b}$$

with

$$p_z = \frac{2\pi}{L} n \qquad n = 0, \pm 1, \pm 2, \ldots.$$

Using (13), (12), (10), (3), (4), (5) and performing the corresponding integration, in the limit $L \to \infty$ we obtained that the reflection coefficient is of the form

$$R(\boldsymbol{k}_\parallel, k_z^n(E, \boldsymbol{k}_\parallel); \boldsymbol{k}_\parallel, k_z^p(E, \boldsymbol{k}_\parallel)) = \left|\frac{b}{a}\right|^2 \tag{14}$$

and the non-zero transition probabilities are only for transitions between states with the same parallel with the interface component of the wave vector. The wave vector of an incident electron determines unambiguously the wave vector of a reflected electron and so also the possible reflection channels.

Now we need to evaluate the coefficients a and b appearing in the function $f_>$ for $z < 0$ (equation (12b)). The function $f_>$ obeys the modified equation (7) and satisfies the boundary condition (11b). From the character of equation (7) (with zero right-hand side) it follows that the functions $f_>(E, \boldsymbol{k}_\parallel; z)$ and $D_z(\boldsymbol{k}_\parallel, z) f_>(E, \boldsymbol{k}_\parallel; z)$ are continuous functions of the coordinate z. We construct a two-component column vector with the components

$$F_1(E, \boldsymbol{k}_\parallel; z) \equiv f_>(E, \boldsymbol{k}_\parallel; z) \qquad F_2(E, \boldsymbol{k}_\parallel; z) \equiv \frac{\hbar}{\mathrm{i}v_z^0} D_z(\boldsymbol{k}_\parallel, z) f_>(E, \boldsymbol{k}_\parallel; z). \tag{15}$$

The pre-factor in the definition of F_2 ensures that the two vector components have the same physical dimensions. Considering (7), we find that the $\boldsymbol{F}$-vector obeys the equation

$$\frac{\partial}{\partial z} F(E, \boldsymbol{k}_\parallel; z) = \mathrm{i}U(E, \boldsymbol{k}_\parallel; z) F(E, \boldsymbol{k}_\parallel; z). \tag{16}$$

The $\mathbf{U}$ matrix is of the order 2×2 and has the following components:

$$U_{11}(E, \boldsymbol{k}_\parallel; z) = U_{22}(E, \boldsymbol{k}_\parallel; z) \equiv -m_{zz}(z)\left(\frac{k_x}{m_{zx}(z)} + \frac{k_y}{m_{zy}(z)}\right) \tag{17a}$$

$$U_{12}(E, \boldsymbol{k}_\parallel; z) \equiv \frac{v_z^0 m_{zz}(z)}{\hbar} \tag{17b}$$

$$U_{21}(E, \boldsymbol{k}_\parallel; z) \equiv \frac{\hbar}{v_z^0}\left[\frac{2}{\hbar^2}(E - E_\parallel(\boldsymbol{k}_\parallel, z) - U(z) - \Sigma(E, z)) + m_{zz}(z)\left(\frac{k_x}{m_{zx}(z)} + \frac{k_y}{m_{zy}(z)}\right)^2\right]. \tag{17c}$$

The solution of equation (16) can be written in the form

$$\boldsymbol{F}(E, \boldsymbol{k}_\parallel; z) = \boldsymbol{\alpha}(E, \boldsymbol{k}_\parallel; z, z')\boldsymbol{F}(E, \boldsymbol{k}_\parallel; z'). \tag{18}$$

This expression connects the values of the $\boldsymbol{F}$-vector at two points. We can assume that the value of $\boldsymbol{F}(E, \boldsymbol{k}_\parallel; z')$ is known and serves as the 'boundary condition'. So, using (18), we are able to evaluate the $\boldsymbol{F}$-vector at any other point. From (18) it follows that the matrix $\boldsymbol{\alpha}$ has the following properties:

(1) $\boldsymbol{\alpha}(E, \boldsymbol{k}_\parallel; z, z) = \mathbf{1}$ and
(2) $\boldsymbol{\alpha}(E, \boldsymbol{k}_\parallel; z, z') = \boldsymbol{\alpha}(E, \boldsymbol{k}_\parallel; z, z'')\boldsymbol{\alpha}(E, \boldsymbol{k}_\parallel; z'', z')$.

Using (16), the matrix $\boldsymbol{\alpha}$ can be formally written in the form

$$\boldsymbol{\alpha}(E, \boldsymbol{k}_\parallel; z, z') \equiv \exp\left[-\mathrm{i}\int_{z'}^{z} \mathrm{d}u \left(k_x \frac{m_{zz}(u)}{m_{zx}(u)} + k_y \frac{m_{zz}(u)}{m_{zx}(u)}\right)\right] \mathbf{A}(E, \boldsymbol{k}_\parallel; z, z') \tag{19a}$$

and for $z \geqslant z'$

$$\mathbf{A}(E, \boldsymbol{k}_\parallel; z, z') \equiv T_z \exp\left[\mathrm{i}\int_{z'}^{z} \mathrm{d}u \begin{pmatrix} 0 & U_{12}(E, \boldsymbol{k}_\parallel; u) \\ U_{21}(E, \boldsymbol{k}_\parallel; u) & 0 \end{pmatrix}\right]. \tag{19b}$$

Here T_z represents the space-ordering operation. When applied to a product of matrices it arranges them from the right to the left in the order of increasing z, i.e. it puts the matrices with larger z to the left of those with smaller z. So, the matrix with the smallest z appears on the right-hand margin of the chain of matrices and that with the largest z appears on the left-hand margin.

The coefficients a and b (or more accurately the ratio b/a) can be expressed in terms of the matrix $\boldsymbol{\alpha}$ using equation (18). To do this, z' is chosen deep in the ordinary-metal electrode ($z' < 0$) ($f_>(E, \boldsymbol{k}_\parallel; z')$ has the form (12*b*)) and z deep in the electrode made of the metal being investigated ($z > Z$) (the function $f_>(E, \boldsymbol{k}_\parallel; z)$ has the form of a wave propagating from the interface).

As $|b/a|^2$ is the reflection coefficient and there is only one reflection channel, the transmission coefficient is evaluated as $1 - |b/a|^2$. After some algebraic operations, the following expression is obtained for the transmission coefficient of an electron incident in the state characterized by the wave vector $\boldsymbol{k} = (\boldsymbol{k}_\parallel, k_z^p(E, \boldsymbol{k}_\parallel))$:

$$T(\boldsymbol{k}_\parallel, k_z^p(E, \boldsymbol{k}_\parallel)) = 2\Big/\left(1 - \frac{\mathrm{Tr}[\mathbf{A}^+(E, \boldsymbol{k}_\parallel; Z, 0)\mathbf{V}(E, \boldsymbol{k}_\parallel)\mathbf{A}(E, \boldsymbol{k}_\parallel; Z, 0)]}{\mathrm{Tr}[\boldsymbol{\tau}\mathbf{A}^+(E, \boldsymbol{k}_\parallel; Z, 0)\mathbf{V}(E, \boldsymbol{k}_\parallel)\mathbf{A}(E, \boldsymbol{k}_\parallel; Z, 0)]}\right). \tag{20}$$

Here

$$\boldsymbol{\tau} \equiv \begin{pmatrix} 0 & 1 \\ 1 & 0 \end{pmatrix} \qquad \mathbf{V}(E, \boldsymbol{k}_\parallel) \equiv \begin{pmatrix} |w/v_z^0|^2 & -w^*/v_z^0 \\ -w/v_z^0 & 1 \end{pmatrix}$$

and

$$w(E, \boldsymbol{k}_\parallel) \equiv \hbar\left(\frac{k_x}{m_{zx}(\infty)} + \frac{k_y}{m_{zy}(\infty)} + \frac{Q^p}{m_{zz}(\infty)}\right).$$

Q^p is the solution of the equation

$$\frac{k_x}{m_{zx}(\infty)} + \frac{k_y}{m_{zy}(\infty)} + \frac{Q^p}{m_{zz}(\infty)} = \sqrt{\frac{v_z^0 U_{21}(E, \boldsymbol{k}_\parallel; \infty)}{\hbar m_{zz}(\infty)}}$$

with $\mathrm{Im}\, Q^p \geqslant 0$.

Tr($\mathbf{A}$) means the sum of diagonal elements of matrix $\mathbf{A}$; $\mathbf{A}^+$ is the Hermitian conjugate of matrix $\mathbf{A}$.

As is seen from (20), in the resultant expression there are only $\mathbf{A}$ matrices for the region $0 \leqslant z \leqslant Z$, i.e. for the sample region with varying parameters. So, the result is independent of the particular choice of the points z' and z used in the intermediate stages

of the deductive process. This is due to fact that the contributions to $\mathbf{A}$ matrices from the 'constant-parameter tails' (i.e. regions with $z < 0$ and $z > Z$), appearing in the intermediate stages, cancel one another out in the final expression (20).

3. Discussion and conclusions

The aim of the work presented in this article was to find the expression for the transmission coefficient, i.e. the probability of transmission of an electron from an ordinary-metal electrode through the planar interlayer region into the electrode made of the material being investigated, for the case of inelastic transport. Inelasticity is characterized by a finite quasiparticle lifetime in the interlayer region and in the electrode made of the material being investigated, represented by the finite imaginary part of the retarded self-energy.

In the general derived expression (20), the crucial role is played by the matrix (19*b*) assigned to the sample region with varying parameters. This matrix is unambiguously determined by the functional shapes of the relevant parameters. In the case presented, these parameters are the reciprocal-effective-mass tensor, the one-electron potential energy and the one-electron retarded self-energy.

Unfortunately, in general, the relevant matrix (19*b*) cannot be expressed in an explicit analytical form. But its properties (in particular the property 2) enable us to write this matrix as a product of 'partial' matrices assigned to the individual sub-layers (real or imaginary) constituting the relevant sample region. If the 'division' of the region into sub-layers is sufficiently fine, i.e. the number of sub-layers is large enough, we can treat each sub-layer as a region of constant parameters. In this case each partial matrix has the form

$$\mathbf{A}_j = \begin{pmatrix} \cos\sqrt{U_{12}^j U_{21}^j}\, l_j & \mathrm{i}\dfrac{U_{12}^j}{\sqrt{U_{12}^j U_{21}^j}} \sin\sqrt{U_{12}^j U_{21}^j}\, l_j \\ \dfrac{\mathrm{i}U_{21}^j}{\sqrt{U_{12}^j U_{21}^j}} \sin\sqrt{U_{12}^j U_{21}^j}\, l_j & \cos\sqrt{U_{12}^j U_{21}^j}\, l_j \end{pmatrix}. \tag{21}$$

The quantities U_{12}^j and U_{21}^j are defined by equations (17*b*) and (17*c*) with constant parameters introduced that relate to the jth sub-layer, and l_j is the thickness of this sub-layer. The total matrix can be expressed as

$$\mathbf{A} = \mathbf{A}_n \mathbf{A}_{n-1} \cdots \mathbf{A}_2 \mathbf{A}_1. \tag{22}$$

The sub-layers are numbered in the direction of motion of a transmitted electron.

If the imaginary part of the self-energy vanishes, i.e. we are dealing with elastic transport, expression (20) can be transformed into the simpler form

$$T(\boldsymbol{k}_\parallel, k_z^p(E, \boldsymbol{k}_\parallel)) = 4 \Big/ \left\{ 2 + \mathrm{Tr}\left[\begin{pmatrix} w/v_z^0 & 0 \\ 0 & v_z^0/w \end{pmatrix} \mathbf{A}(E, \boldsymbol{k}_\parallel; Z, 0) \mathbf{A}^+(E, \boldsymbol{k}_\parallel; Z, 0) \right] \right\}. \tag{23}$$

The quantity w is defined above.

To demonstrate the use of the derived method for evaluating the transmission coefficient, the differential conductance for a tunnelling contact between an ordinary metal and an anisotropic MFL metal is calculated.

We consider the case in which the Fermi energy E_F of an ordinary metal is sufficiently high compared with the range of the applied voltage V_m ($E_F \gg eV_m$) and the tunnelling regime is well established ($U_B \gg eV_m$, where U_B is the height of a rectangular potential

barrier). Then the low-temperature differential conductance $G_D(V) \equiv \mathrm{d}I(V)/\mathrm{d}V$ can be expressed as [14]

$$\frac{G_D(V)}{G_D(0)} = \left(\int_0^{\pi/2} \mathrm{d}\theta \ \sin\theta \int_0^{2\pi} \mathrm{d}\varphi \ (\cos\theta) T(\boldsymbol{k}_{F\parallel}, k_Z^P(E_F + eV, \boldsymbol{k}_{F\parallel}))\right) \times \left(\int_0^{\pi/2} \mathrm{d}\theta \ \sin\theta \int_0^{2\pi} \mathrm{d}\varphi \ (\cos\theta) T(\boldsymbol{k}_F)\right)^{-1}. \tag{24}$$

Here the transmission coefficient T corresponds to the situation without an applied bias (zero potential energy due to external fields). θ and φ are the polar and azimuthal angles of the incident-electron wave vector (the z-axis serves as a polar axis and the x-axis as an azimuthal axis); $\boldsymbol{k}_F$ is the Fermi wave vector of an ordinary-metal electron. To deal with electrons transmitted from an ordinary metal into a MFL metal (the case investigated in this article), we take into account only the positive bias (a positive bias means that the MFL is positive).

At low temperatures, the MFL is characterized by a one-electron retarded self-energy of the form [7, 8]

$$\Sigma(\boldsymbol{k}, E_F + \varepsilon) = \lambda\left(\varepsilon \ln\frac{|\varepsilon|}{\varepsilon_c} - \mathrm{i}\frac{\pi}{2}|\varepsilon|\right). \tag{25}$$

Here λ is a coupling constant and ε_c is a high-energy cut-off.

The real Cu–O-based high-T_c superconductors are anisotropic 'layered' structures with an isotropic effective mass m_{ab} within the a–b planes and a different and much higher effective mass m_c in the direction of the c-axis, perpendicular to a–b planes (see, e.g., [15, 16]). Moreover, the normal-state conductivity is hole like and the charge-carrier concentration is much lower than in an ordinary metal. To model this situation in a simple way, we assume that in the MFL the Fermi level is near the top of the conduction band E_0 ($E_0 - E_F \sim 0.1$ eV; low 'hole' concentration) and the conduction electrons have negative effective masses. So, the 'band' electronic dispersion relation in the MFL is chosen in the form

$$\varepsilon(\boldsymbol{k}) = E_0 - \frac{\hbar^2}{2}\boldsymbol{k} \cdot \frac{1}{\mathbf{m}(\infty)} \cdot \boldsymbol{k}. \tag{26}$$

The components of the symmetric REM tensor are

$$\begin{aligned} \frac{1}{m_{xx}(\infty)} &= \frac{1}{m_{ab}} & \frac{1}{m_{yy}(\infty)} &= \frac{\sin^2\gamma}{m_c} + \frac{\cos^2\gamma}{m_{ab}} \\ \frac{1}{m_{zz}(\infty)} &= \frac{\sin^2\gamma}{m_{ab}} + \frac{\cos^2\gamma}{m_c} & \frac{1}{m_{xy}(\infty)} &= \sin\gamma\cos\gamma\left(\frac{1}{m_{ab}} - \frac{1}{m_c}\right). \end{aligned} \tag{27}$$

The other elements are zero. γ is the angle between the c-axis and the z-axis; the x-axis is chosen to lie in the a–b plane.

In this section we simply aim to illustrate the method used for calculating the transmission coefficient, not to verify that the MFL is a suitable model for the normal state of high-T_c superconductors or to search for optimum model parameters. So we accept without discussion some of the values presented by other authors [15–17] ($\lambda = 0.3$, $\varepsilon_c = 0.1$ eV, $E_0 = E_F + 0.1$ eV, $m_{ab} = (5/6)m_e$, $m_c = (100/6)m_e$; m_e is the free-electron mass). For the ordinary metal we use the parameters corresponding to Ag ($E_F = 5.48$ eV, $k_F = 12$ nm^{-1}) and an isotropic effective mass $m_0 = m_e$.

For particular calculations we use, for simplicity, a slightly artificial model with a sharp interface between a high rectangular potential barrier and a MFL metal as regards the REM

tensor but not the self-energy. The MFL REM tensor of the form (27) is constant up to the interface; the effective mass in the barrier is the same as in the ordinary-metal electrode and is also constant up to the interface. For the self-energy the interface is not sharp, in the sense that the coupling constant λ can be a function of the distance from the interface and reach its bulk value at a distance $L \geqslant 0$.

Calculations were performed for various situations. The differential conductance was calculated according to (24) and the transmission coefficients according to (20)–(22). The region with the parameter λ varying was divided into ten sub-regions. This degree of division was found to be sufficient; finer division does not lead to substantial changes.

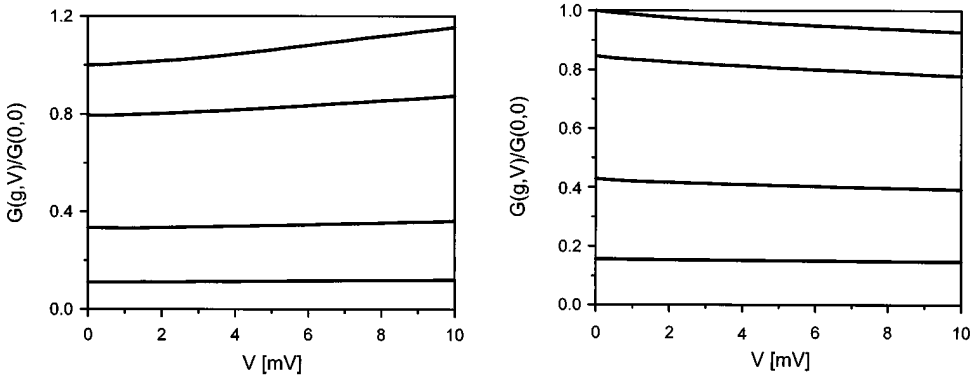

Figure 1. The normalized differential conductance versus the applied voltage for a contact with sharp interfaces. The curves presented correspond to situations in which the barrier thicknesses are 0.1 nm (a) and 1 nm (b) and with the following values of the angle γ ($g \equiv \cos\gamma$) between the MFL c-axis and the normal to the contact (from top to bottom): 90° (tunnelling in the a–b plane direction), 60°, 30° and 0° (tunnelling in the c-axis direction).

First, the effect of the barrier thickness on the differential conductance was investigated for the case of a sharp 'self-energy' interface (the self-energy is constant up to the interface). For high ($U = 2E_F$) thin barriers, the $G_D(V)$s are nearly linear functions of V with positive slope for all angles γ between the MFL c-axis and the normal to the interface. The slopes, as well as the absolute values of the differential conductance, decrease with decreasing angle γ. So, the highest slope and differential-conductance values are for tunnelling in the a–b plane direction, the lowest for tunnelling in the c-axis direction. But as the barrier thickness increases, the slopes of the $G_D(V)$ curves decrease and finally become negative. This effect is illustrated in figures 1(a) and 1(b).

Such behaviour of the differential conductance is caused by two different processes. For electrons incident almost vertically onto the clear surface of the MFL, with our parameters, the transmission probability decreases with increasing energy due to the increase of the difference between the wave vectors of the incident and transmitted electrons (see dispersion relation (26)) (figure 2). This tendency is only slightly affected by the many-particle effects in the relevant energy region. On the other hand, for electrons incident non-vertically, the transmission probability (vanishing at the Fermi level) increases with increasing energy just due to the inelastic many-particle effects (e.g. the finite lifetime of an electron in a given state) (figure 3).

The thin potential barrier in front of the MFL surface transmits electrons incident at various angles with nearly equal probabilities. Electrons incident non-vertically can be

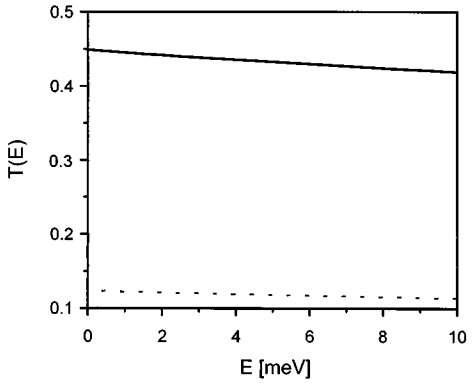

Figure 2. The transmission coefficient versus the energy for an electron incident onto a clear sharp interface perpendicularly. The curves presented correspond to tunnelling in the *a–b* plane direction (solid line) and in the *c*-axis direction (dashed line). The energy is measured from the Fermi level.

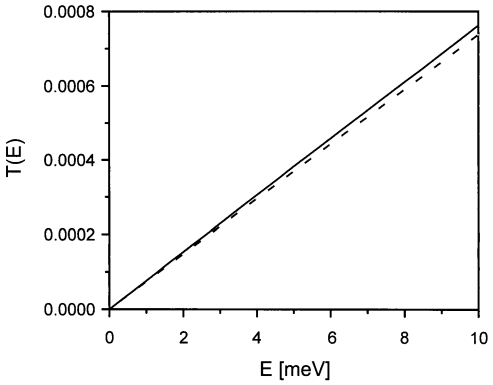

Figure 3. The transmission coefficient versus the energy for an electron incident onto a clear sharp interface non-perpendicularly. The direction of incidence is characterized by the polar angle 60° and azimuthal angle 0° (the normal to the interface serves as a polar axis and the azimuthal axis is perpendicular to the normal to the interface as well as to the MFL *c*-axis). The curves presented correspond to electrode configurations characteristic of tunnelling in the *a–b* plane direction (solid line) and the *c*-axis direction (dashed line). The energy is measured from the Fermi level.

revealed in the resulting conductance and their contribution outweighs the contribution of electrons incident nearly vertically. So, in this case the differential conductance is an increasing function of the voltage.

On the other hand, a thick barrier strongly reduces the transmission probabilities for electrons incident on the barrier non-vertically. So, only the electrons incident nearly vertically are manifested and the differential conductance is a decreasing function of the voltage.

A similar effect is also caused by suppressing the inelastic many-particle effects (the imaginary part of the self-energy) near the MFL surface. The MFL region with a suppressed self-energy imaginary part acts as an additional effective barrier suppressing the contribution of 'non-vertical' electrons. This situation is illustrated in figures 4 and 5.

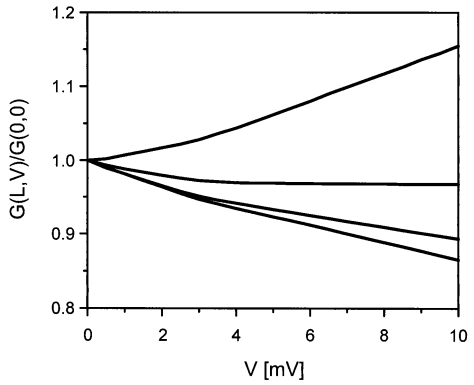

Figure 4. The normalized differential conductance versus the applied voltage for a contact containing a sub-layer with a linearly increasing coupling-constant value. The curves presented correspond to tunnelling in the *a–b* plane direction for a barrier thickness of 0.1 nm and with the following values of the sub-layer thickness L (from top to bottom): 0 nm (the sharp interface), 0.2 nm, 0.5 nm and 1 nm.

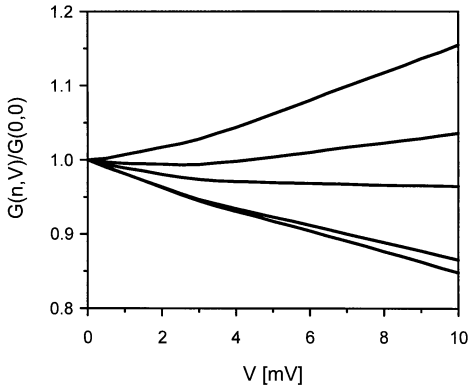

Figure 5. The normalized differential conductance versus the applied voltage for a contact containing a sub-layer with a coupling-constant value increasing according to a power law. The curves presented correspond to tunnelling in the *a–b* plane direction for a barrier thickness of 0.1 nm, a sub-layer thickness of $L = 1$ nm and with the following values of the exponent n appearing in the power law $(z/L)^n \lambda_{bulk}$ describing the coupling-constant increase (from top to bottom): 0 (the sharp interface), 0.25, 0.5, 1 and 4.

Figure 4 presents the differential conductances for contacts with linearly increasing self-energy intensity (coupling constant λ), from zero to the bulk value, for various rates of increase, i.e. various lengths of regions with varying self-energy. The slope of the $G_D(V)$ curve decreases with increasing length of this region.

In figure 5, the differential conductances for various functional shapes of the self-energy increase in regions of the same length are presented. We again see that the slope decreases with decreasing rate of the coupling-constant increase near the surface, i.e. with extension of the region of suppressed self-energy values.

Differential-conductance curves for tunnelling contact between an ordinary metal and a MFL, similar to those in figures 1(a) and 1(b), were calculated in [17] by another method based on the tunnelling Hamiltonian approach. In that article, tunnelling in the *c*-axis

direction was investigated. Dispersion along the c-axis was neglected, i.e. $1/m_c = 0$, and within the a–b plane the electron-like parabolic band dispersion relation was used (in contrast to our hole-like dispersion relation (26)). In that case the positive slope of the $G_D(V)$ curves decreased with decreasing barrier thickness, in contrast with our results. A small negative slope of the $G_D(V)$ curves was expected for tunnelling in the a–b plane direction.

In [18], tunnelling measurements on cubic Ba–Pb(K)–Bi–O superconductors were presented. The normal state of these materials is also expected to possess marginal-Fermi-liquid character. The differential-conductance curves presented in [18] (all with positive slope) are similar to our dependencies shown in figure 1(a). Discussion of the applicability of the marginal Fermi liquid as a model for the normal state of Cu–O-based or Bi–O-based superconductors, as well as the search for optimal MFL parameters to fit the experimental data, are beyond the scope of this article. But the derived method for calculating the transmission coefficient (and so also the differential conductance) represents a good starting point for our further work in this field.

Acknowledgment

The author is grateful to the Slovak Grant Agency for Science (grant No 2/1359/97) for partial support of this work.

References

[1] Landauer R 1990 *Analogies in Optics and Micro Electronics* ed W van Haeringen and D Lenstra (Dordrecht: Kluwer) pp 243–57
[2] Büttiker M 1990 *Electronic Properties of Multilayers and Low-Dimensional Semiconductor Structures* ed J M Chamberlain (New York: Plenum) pp 51–73
[3] Datta S and McLennan M J 1990 *Rep. Prog. Phys.* **53** 1003
[4] Van de Leemput L E C and Van Kempen H 1992 *Rep. Prog. Phys.* **55** 1165
[5] Kirtley J R 1990 *Int. J. Mod. Phys.* B **4** 201
[6] Zebda Y and Kan'an A M 1992 *J. Appl. Phys.* **72** 559
[7] Varma C M, Littlewood P B, Schmitt-Rink S, Abrahams E and Ruckenstein A E 1989 *Phys. Rev. Lett.* **63** 1996
[8] Varma C M 1989 *Int. J. Mod. Phys.* B **3** 2083
[9] Bonch-Bruevich V L and Tyablikov S V 1961 *Green's Functions Method in Statistical Mechanics* (Moscow: Fizmatgiz) (in Russian)
[10] Kupka M 1996 *Solid State Commun.* **98** 869
[11] Varma C M 1985 *Phys. Rev. Lett.* **55** 2723
[12] Abrikosov A A, Gor'kov L P and Dzyaloshinskii I Ye 1965 *Quantum Field Theoretical Methods in Statistical Physics* (Oxford: Pergamon)
[13] Lukes T 1969 *Solid State Theory. Methods and Applications* ed P T Landsberg (New York: Wiley) pp 405–506
[14] Kupka M 1991 *Phys. Lett.* **154A** 54
[15] Schneider T and Frick M 1990 *Earlier and Recent Aspects of Superconductivity* ed J G Bednorz and K A Müller (Berlin: Springer) pp 501–17
[16] Kresin V Z and Wolf S A 1990 *Phys. Rev.* B **41** 4278
[17] Littlewood P B and Varma C M 1992 *Phys. Rev.* B **45** 12 636
[18] Sharifi F, Pargellis A and Dynes R C 1991 *Phys. Rev. Lett.* **67** 509